J. Cent. South Univ. (2022) 29: 2357−2376
DOI: https://doi.org/10.1007/s11771-022-5073-y

Springer

Comparison of life cycle performance of distributed energy system and conventional energy system for district heating and cooling in China

LIU Chang-rong(刘畅荣)[1], TANG Yi-fang(唐艺芳)[2], WANG Han-qing(王汉青)[1,3], LIU Zhi-qiang(刘志强)[1], YANG Sheng(杨声)[1]*, LI Chao-jun(李朝军)[4], JIN Wen-ting(金文婷)[4]

1. School of Energy Science and Engineering, Central South University, Changsha 410083, China;
2. School of Civil Engineering, Hunan University of Science and Technology, Xiangtan 411201, China;
3. School of Civil Engineering, Central South University of Forestry and Technology, Changsha 410004, China;
4. School of Civil Engineering, Hunan University of Technology, Zhuzhou 412007, China

Abstract: The distributed energy system has achieved significant attention in respect of its application for single-building cooling and heating. Researching on the life cycle environmental impact of distributed energy systems (DES) is of great significance to encourage and guide the development of DES in China. However, the environmental performance of distributed energy systems in a building cooling and heating has not yet been carefully analyzed. In this study, based on the standards of ISO14040-2006 and ISO14044-2006, a life-cycle assessment (LCA) of a DES was conducted to quantify its environmental impact and a conventional energy system (CES) was used as the benchmark. GaBi 8 software was used for the LCA. And the Centre of Environmental Science (CML) method and Eco-indicator 99 (EI 99) method were used for environmental impact assessment of midpoint and endpoint levels respectively. The results indicated that the DES showed a better life-cycle performance in the usage phase compared to the CES. The life-cycle performance of the DES was better than that of the CES both at the midpoint and endpoint levels in view of the whole lifespan. It is because the CES to DES indicator ratios for acidification potential, eutrophication potential, and global warming potential are 1.5, 1.5, and 1.6, respectively at the midpoint level. And about the two types of impact indicators of ecosystem quality and human health at the endpoint level, the CES and DES ratios of the other indicators are greater than 1 excepting the carcinogenicity and ozone depletion indicators. The human health threat for the DES was mainly caused by energy consumption during the usage phase. A sensitivity analysis showed that the climate change and inhalable inorganic matter varied by 1.3% and 6.1% as the electricity increased by 10%. When the natural gas increased by 10%, the climate change and inhalable inorganic matter increased by 6.3% and 3.4%, respectively. The human health threat and environmental damage caused by the DES could be significantly reduced by the optimization of natural gas and electricity consumption.

Key words: life-cycle assessment; distributed energy system; conventional energy system; building cooling and heating; environmental impact

Cite this article as: LIU Chang-rong, TANG Yi-fang, WANG Han-qing, LIU Zhi-qiang, YANG Sheng, LI Chao-jun, JIN Wen-ting. Comparison of life cycle performance of distributed energy system and conventional energy system for district heating and cooling in China [J]. Journal of Central South University, 2022, 29(7): 2357−2376. DOI: https://doi.org/10.1007/s11771-022-5073-y.

Foundation item: Projects(51676209, 22008265) supported by the National Natural Science Foundation of China; Projects(2020JJ6072, 2021JJ50007) supported by the Hunan Province Natural Science Foundation, China
Received date: 2021-07-17; **Accepted date:** 2021-12-05
Corresponding author: YANG Sheng, PhD, Associate Professor; E-mail: ceshyang@csu.edu.cn; ORCID: https://orcid.org/0000-0002-3119-8131

1 Introduction

The energy consumption of buildings accounts for approximately 35% of the total energy consumption in China [1]. The building energy demands mainly consist of district cooling, heating, and hot water [2]. In a conventional energy system, the district cooling and heating are usually supplied by electricity from the grid and hot water is supplied by natural gas combustion. A distributed energy system (DES) is an energy-efficient alternative that can replace a conventional energy system for building energy supplementation [3]. The DES is a promising method to meet increasing energy consumption demands, which could not only improve renewable energy utilization, but also solve the intermittence problem of renewable energy utilization [4−5].

Solar energy is a renewable energy resource that has become an important energy source for DES [6]. Solar-assisted DES has the advantages of lower emissions and energy consumption than fossil fuel energy systems and lower cost than solar-only energy systems [7]. FANI et al [8] proposed a solar-assisted DES for district heating and cooling for an educational office building and analyzed the 3E (economic, energetic, and environmental) performance. LIU et al [9] proposed a new solar-assisted DES and investigated the performance of the new system. Their results show that, compared with the conventional CCHP systems, the efficiency of the new system can reach up to 39.23%. YILMAZ [10] investigated a novel assisted DES to produce district heating and cooling, power, clean hydrogen, and freshwater and evaluated the thermodynamic performance. The results show that the overall energy efficiency and exergy efficiency of the proposed multi-generation system were calculated as 78.93% and 47.56%, respectively, at 800 W/m^2 solar radiation.

However, the solar-only DES cannot operate continuously due to the fluctuation and intermittence of solar energy. Geothermal energy is considered an effective renewable resource that could solve the fluctuation problem [11]. Ground reversible heat pumps are driven by geothermal energy and have been developed in many countries for district heating and cooling [12]. The solar-assisted DES integrated with a ground-source heat pump applied for district heating and cooling has been studied by many researchers [13−16]. It was found that ground temperature might be subject to fluctuations due to the overuse of geothermal energy, which would result in the lower efficiency of the ground source heat pump [17]. YUAN et al [18] proposed a control strategy for thermal energy storage systems and the distributed energy system. Their results show that the proposed strategy can improve the surplus energy utilization rate by 29.3% and the primary energy efficiency by 2.9%; additionally, the payback period can be decreased from 3.6 years to 1.9 years. The solar energy can be stored underground in the summer and extracted in the winter. Solar energy is used in the daytime and geothermal energy is supplied during the night. The annual geothermal energy could be balanced and the intermittence problem of solar energy could be solved. The DES combined solar energy and geothermal energy could be operated continuously.

Life-cycle assessment (LCA) is regarded as an important tool for the evaluation of environmental impacts [19]. JING et al [20] analyzed the environmental and energy benefits of BCHP (building cooling, heating, and power) using the LCA method. Their results show that BCHP using the strategy of following the electricity load has the best performance. ZHANG et al [21] optimally designed BCHP microgrids considering economic and environmental sustainability and investigated the LCA performance of the system. Their results show that a microgrid with a cooling, heating, and power system is an environmental-friendly solution for different group users. WANG et al [2] optimized a combined district heating, cooling, and power DES based on the life-cycle performance. The results indicate that FTL strategy is superior to FEL strategy at taking the environmental compensation of surplus products from the hybrid CCHP system into consideration. ANASTASELOS et al [22] evaluated the energy systems in residential buildings using LCA. Their results show that the energy system structure has a significant impact on the total environmental impact. OREGI et al [23] established a state-of-the-art LCA methodology for building rehabilitation and considered the environmental impact of life-cycle stages. MOSLEHI et al [24] presented an LCA methodology to assess integrated energy systems that can evaluate the cogeneration system in real-time. ALBERTÍ et al [25] conducted an assessment of a solar-thermal system and natural gas heating system using LCA. Their results show that the solar system produced a markedly better performance in respect of global warming and a poor performance in terms of acidification and eutrophication. Furthermore, HAJARE et al [26] explored building energy-efficiency strategy assessment by integrating life-cycle cost analysis and energy simulation. The results show a 13.5% saving in terms of the building cost, employing a combination of passive design and active strategies.

Literature surveys show that few studies have investigated the life-cycle performance of DES integrated with solar and geothermal energy for building cooling and heating in China. In this study, a conventional energy system supplied by natural gas and electricity was used as the benchmark. The originality of this work is its quantification of the environmental impacts of DES using the LCA method, which can encourage and guide the development of distributed energy systems in China. The environmental impacts were investigated in terms of acidification, eutrophication, human toxicity, freshwater aquatic ecotoxicity, terrestrial ecotoxicity, global warming, ozone layer depletion, and photochemical ozone creation potential. In addition, the hots-pot and sensitivity of the DES were analyzed for identifying the phases causing significant environmental impacts.

2 Methods

LCA is used to evaluate and quantify the environmental impact of a process or product from a 'cradle to grave' perspective, which can provide potential strategies to improve the environmental performance of a process or product [27]. According to the standards ISO14040-2006 and ISO14044-2006 [28−29], the LCA method is used to comprehensively compare a DES and a CES for the cooling and heating of a single building. GaBi 8 software was used for the LCA. The GaBi software database is the leading LCA data source in the market and provides an environmental overview of more than 10000 materials and processes [30]. It was developed by the Institutfur Kunstoffprufungund Kunst-stoffkunde in Germany. Additionally, its databases include GaBi databases, a self-built PE International database, the Ecoinvent database in Switzerland, and the life-cycle inventory analysis (LCI) database in the United States [31]. The Centre of Environmental Science (CML) method and Eco-indicator 99 (EI 99) method were used for environmental impact assessment during the LCA. The CML method [32−33] was first used by the Environmental Science Center of Leiden University in the Netherlands in 1992. This method is a typical intermediate impact-type method, covering 10 required impact types. In this paper, the CML method was used for the midpoint environmental impact assessment. The EI 99 method [34−35], proposed by Goedkoop and Spriensma as a new LCA in 1999, is a typical damage orientated approach for 'end point'. It quantifies environmental impact tracking to the end of the impact mechanism for evaluation, which is conducive to revealing the objective nature and ultimate harmfulness of environmental problems and is more suitable for terminal impact evaluation.

2.1 Goal and scope

2.1.1 Goal

The goals of LCA include: 1) to evaluate and compare the environmental impacts; 2) to identify the phases causing significant environmental impacts (i. e., 'hots-pot' identification) in the DES and CES; and 3) to analyze and determine the influence of different variables in the DES on environmental impact indicators.

2.1.2 Scope

This research was to study the DES and CES for building cooling and heating. A public indoor swimming pool was served as the study object. The building was 6.61 m in height and 1143 m^2 in area. The swimming pool had an area of 450 m^2 and a volume of 540 m^3. The energy consumption of the public indoor swimming pool included the use of energy for water heating and building cooling and heating. Building heating and cooling were used to regulate the indoor temperature and relative humidity. The water temperature in swimming pool was kept at 27 °C. The space air temperature was 2 °C higher than the swimming pool temperature, with a relative humidity of 60%.

The function unit was the demanded energy (kW) of the swimming pool load, which includes the hot water load (HWL), air conditioning cooling load (ACL), air conditioning heating load (AHL), and swimming pool electricity load (EL). The whole system considers the energy balance from input to output in the energy utilization system, including the balance of cooling capacity, heat balance, and power balance. The DES consists of a ground reversible heat pump, solar collector, gas boiler, air conditioning unit, water, tank, and heat exchangers. The system boundary of the DES is within the dotted line frame, as shown in Figure 1. The CES consists of an electric chiller, gas boiler, water tank, and heat exchanger. The system boundary of the CES is shown within the dotted line frame in Figure 2. The life-cycle boundary encompasses three phases as the system of construction, usage, and demolition phase. The construction phase of the energy system includes the exploitation, transportation, processing, and manufacture of raw materials. The construction of the indoor swimming pool is the same, so it does not make a difference in the comparison of DES and CES life-cycle performance. The demolition phase encompasses the energy and material consumption and output. In the DES, a solar collector and gas boiler are responsible for the output of the hot water load, an air source heat pump and ground source heat pump output cooling load and heating load, solar panels and wind power output power load, and the insufficient part is provided by the power grid. In the CES, the hot water and heating load are output by the gas boiler, while the cooling and electric load are output by the conventional refrigeration unit and power grid, respectively.

2.2 Data collection

The construction, usage, and demolition phases are considered in the developed methodology. The construction phase considers equipment manufacture, transportation, and system construction. The equipment manufacture takes into account all the manufacturing activities, such as material inputs (e. g. aluminum, copper and steel)

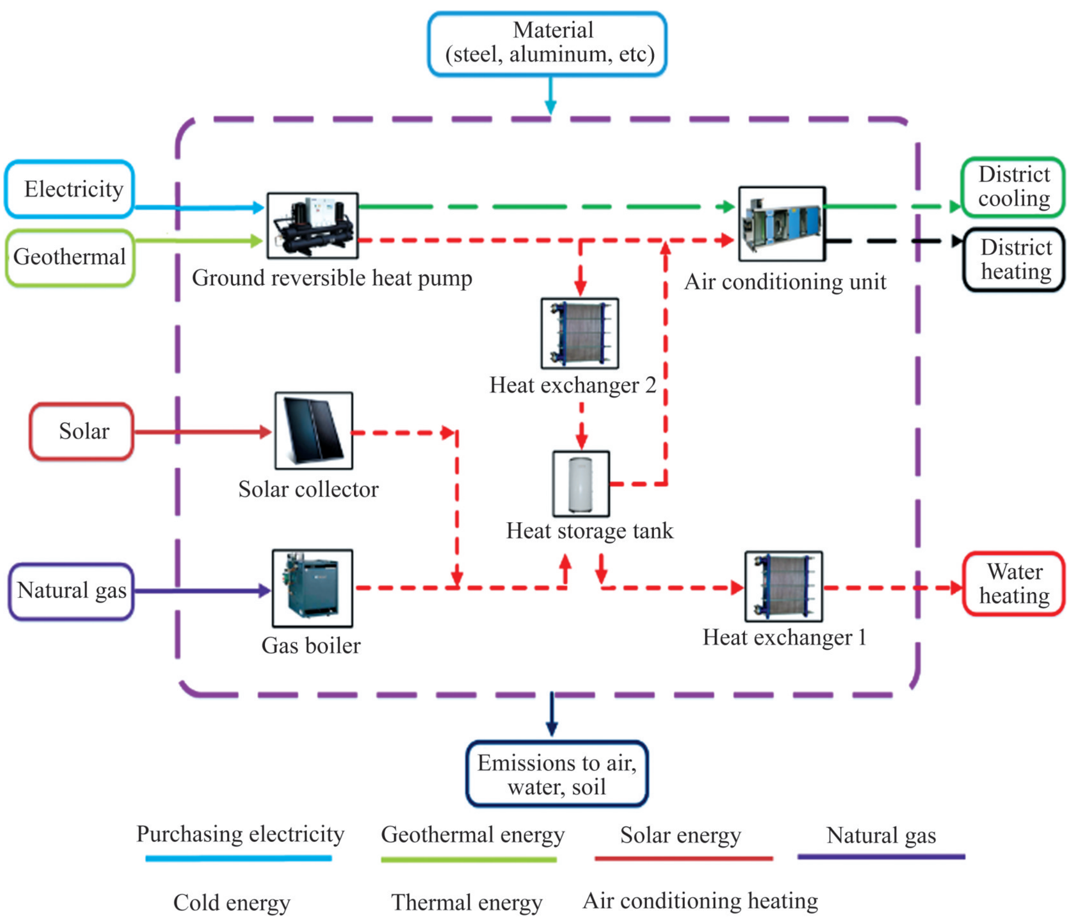

Figure 1 System boundary of the distributed energy system (DES)

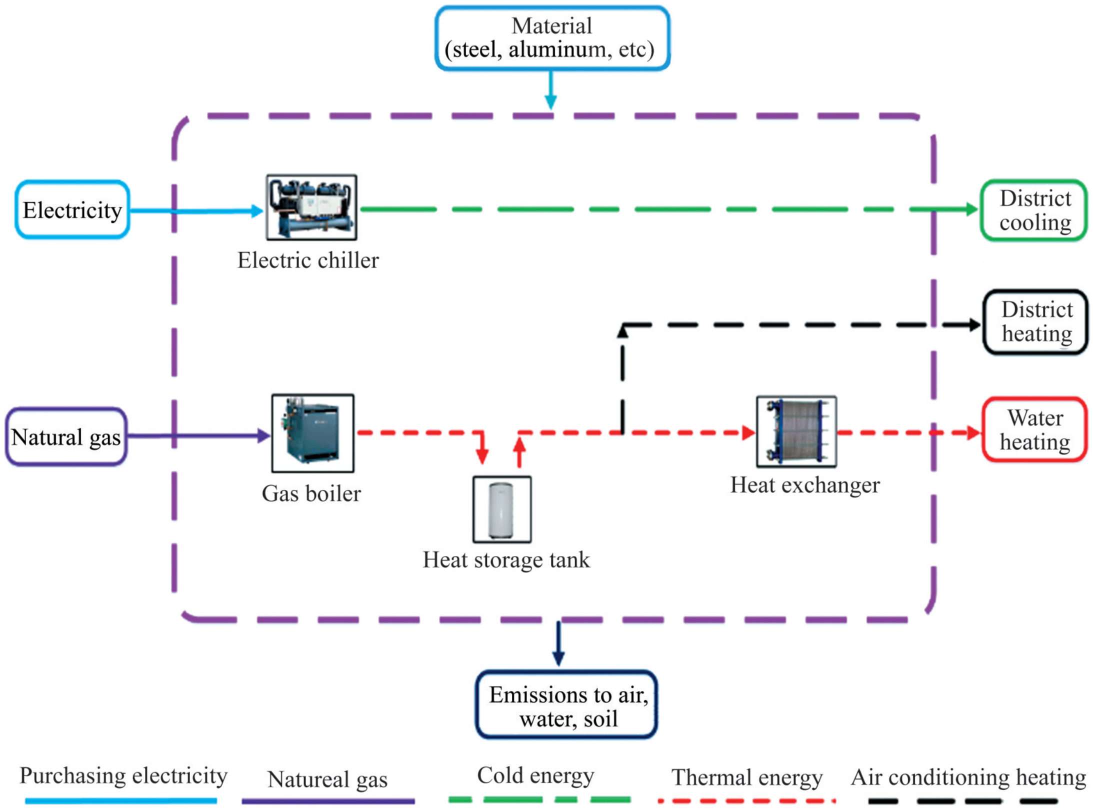

Figure 2 System boundary of the conventional energy system (CES)

and electricity consumed etc. Diesel oil, which is consumed by trucks, is considered in the transportation stage. The system construction uses material, energy, and equipment, which are estimated on the basis of the indoor swimming pool capacity. Natural gas and electricity from the grid are considered in the usage phase, which is a vital phase that influences the life-cycle performance of the system. The project life is assumed to be 20 years. The last phase is the demolition phase. In this phase, all the metals are recovered and the rest materials are landfilled. The mass-energy life cycle inventory for DES and CES is listed in Table A1.

The pollutant emissions investigated in this study include carbon dioxide (CO_2), nitrogen oxide (NO_x), sulfur dioxide (SO_2), particulate matter (PM), etc. The pollutant emissions consist of indirect and direct emissions. The indirect emissions were calculated using the GaBi software database [30]. The direct emissions mainly come from natural gas combustion. The pollutant emissions can be calculated as follows:

$$E_{i,\mathrm{t}}=E_{i,\mathrm{d}}+E_{i,\mathrm{ind}} \tag{1}$$

$$E_{i,\mathrm{ind}}=\sum m_{\mathrm{p},j}\times F_{j,i} \tag{2}$$

where $E_{i,\mathrm{t}}$ represents the total emission of i pollutant during the whole life; $E_{i,\mathrm{d}}$ and $E_{i,\mathrm{ind}}$ are the direct and indirect emission of i pollutant, respectively; j represents life phase (i.e. construction phase, usage phase, and demolition phase); $m_{\mathrm{p},j}$ is the consumption of raw materials and energy; $F_{j,i}$ is the emission factor.

2.3 LCI and life-cycle impact assessment methods

The environmental impacts of the DES and CES at the midpoint and endpoint levels were evaluated and compared in this study. The midpoint level assessment is oriented and targeted towards environmental problems, clarifying the mechanisms existing between the emitted pollutants and environmental damage [36]. However, this assessment neglects the impact of the damage to resources, ecosystems, and humans. The midpoint level environmental impact is assessed using the CML method. The CML method is mainly used in studies analyzing several impact categories [33, 37]. At the midpoint level, eight typical impact categories are selected in the CML method as the indicators, which are used to evaluate and compare the characteristics of DES and CES. The eight indicators are acidification potential (AP), eutrophication potential (EP), human toxicity potential (HTP), freshwater aquatic ecotoxicity potential (FAETP), terrestrial ecotoxicity potential (TETP), global warming potential (GWP), ozone layer depletion potential (ODP), and photochemical ozone creation potential (POCP). They are aimed at the problems of acidification, eutrophication, ecotoxicity, climate change, stratospheric ozone depletion, and photo-oxidant formation [37].

The endpoint level environmental impact is assessed using the EI 99 method [34, 38−39]. The impact of damage to resources, ecosystems, and humans is considered in the EI 99 method, in contrast to the CML method [35]. Hence, the environmental damage to resources, ecosystems, and humans can be evaluated by the EI 99 method [40]. In this study, ecosystem quality and human health were investigated. Eight typical impact categories were selected in the EI 99 method as the indicators, which were used to evaluate and compare the characteristics of DES and CES. The ecosystem quality (EQ) includes two indicators, acidification/eutrophication (AC) and ecotoxicity (EC). Human health (HH) includes six indicators, namely carcinogenic effect (CE), climate change (CC), ozone layer depletion (OLD), radiation (RA), inhalable inorganic matter (IR), and inhalable organic matter (OR), which are focused on the problems of carcinogenic effects on humans, damage caused by climate change, effects caused by ozone layer depletion, effects caused by radiation, respiratory effects caused by inorganic matter, and respiratory effects caused by organic matter, respectively. Disability-adjusted life years (DALYs) are employed to indicate human health, which can be calculated using a person's years of disabled life plus years of life lost. The potentially disappeared fraction (PDF), which is the species richness fraction, is employed to indicate ecosystem quality.

In the process of LCA, the greater these indicators are, the greater the environmental impact of the system is. Conversely, the smaller the index value, the smaller the environmental impact.

3 Results and discussions

3.1 LCI result

The life-cycle inventories of the building cooling and heating using a DES and a CES are presented in Tables A2 and A3. The construction phase, usage phase, and demolition phase of the DES and CES are all included. The material preparation data of DES in the construction stage included the statistics of actual material consumption and some material data were provided by equipment suppliers. The material data of CES were determined by the budget calculation of building material consumption. In the use stage, it was assumed that the annual consumption of natural gas, electricity and tap water is constant. The electricity data were adopted from the GaBi 2018 database [30]. The energy consumption data were determined by TRNSYS simulation, without considering the changes in renewable energy consumption and energy efficiency. The main data of raw materials in the demolition stage were selected from the GaBi 2018 database, ignoring transportation energy consumption. The input and output of materials less than 0.5 kg are not listed in the table. It can be seen that the LCI material types for the DES and CES show basic agreement. There are three types of input, nonrenewable energy, nonrenewable resources, and renewable resources. There are five types of outputs, waste (stock), emissions to air, emissions to fresh water, emissions to sea water, and emissions to industrial soil. The emissions to air contain 12 heavy metals, 4 inorganic substances, particles, and other emissions. Emissions to fresh water include 5 heavy metals, 23 inorganic substances, 4 organic substances, one radioactive substance, and particles. Emissions to sea water include 6 inorganic substances and one organic substance. Emissions to industrial soil include 5 inorganic substances.

3.2 Midpoint analysis

3.2.1 Comparative total impact analysis

The midpoint level life-cycle impact assessment results for the DES and CES are illustrated in Table 1. The environmental impacts of the acidification potential, eutrophication potential, global warming potential, human toxicity potential,

Table 1 Environmental performance at the midpoint level

Category	CES	DES	CES/DES
AP ($SO_{2\,eq}$)/kg	1.43×10^{4}	9.80×10^{3}	1.5
EP(Phosphate $_{eq}$)/kg	1.79×10^{3}	1.16×10^{3}	1.5
FAETP(DCB $_{eq}$)/kg	1.46×10^{4}	1.53×10^{4}	1.0
GWP($CO_{2\,eq}$)/kg	6.04×10^{6}	3.73×10^{6}	1.6
HTP(DCB $_{eq}$)/kg	7.49×10^{5}	6.21×10^{5}	1.2
OLP(R11 $_{eq}$)/kg	3.00×10^{-4}	3.64×10^{-4}	0.8
POCP (Ethene $_{eq}$)/kg	1.16×10^{3}	8.39×10^{2}	1.4
TETP (DCB $_{eq}$)/kg	1.08×10^{4}	1.15×10^{4}	0.9

and photochemical ozone creation potential for the DES are less significant than those for the CES. The CESs to DES indicator ratios for acidification potential, eutrophication potential, and global warming potential are 1.5, 1.5 and 1.6, respectively. The differences in the environmental performance are caused by the energy consumption in the usage phase. The DES is driven by renewable energy, including solar energy and geothermal energy, which results in 51.34% lower natural gas consumption compared with the CES. The freshwater aquatic ecotoxicity potential for the DES and CES is basically same. In addition, the ozone layer depletion potential and terrestrial ecotoxicity potential for DES are greater than those of the CES. The CES/DES indicator ratios for the ozone layer depletion potential and terrestrial ecotoxicity potential are 0.8 and 0.9, respectively. This is mainly caused by the DES using equipment such as a solar collector, ground source heat pump, heat exchanger, and pump in the construction stage, which increases the consumption of materials such as steel, copper, and aluminum and leads to greater emissions of substances such as NO_x and Se.

3.2.2 Comparative phase impact analysis

The midpoint level environmental impacts of DES and CES at different phases are shown in Figure 3. Eight indicators were investigated and compared. It can be seen that the eutrophication, global warming, ozone depletion, photochemical ozone formation, and terrestrial ecotoxicity potential for DES are 90%, 95%, 38%, 100% and 98% larger than those for CES, respectively. All the indicators for the DES are higher than those of the CES in the construction phase. The reason behind these differences is that the DES features more consumables than the CES. However, all the indicators for the DES in the usage stage are changed compared with the CES.

As the use of renewable energy in the DES reduces the consumption of natural gas, the emissions of the DES in the usage stage are reduced and the environmental indicators of the DES in this stage are better than those of the CES. In the demolition stage, the acidification potential, freshwater aquatic ecotoxicity potential, and human toxicity potential all show negative values because of the recovery of steel, copper, and aluminum. The acidification potential, freshwater aquatic ecotoxicity potential, and human toxicity potential for the DES are 60%, 63% and 54% better than those for the CES. In the demolition stage, metal recovery has a positive impact on the environment. The metal recovery for the DES is greater than that for the CES, which results in the environmental benefit of recovery being greater than that for the CES. Moreover, the waste produced in the demolition stage for the DES is greater than that produced for the CES. This causes the environmental impact indicators of the eutrophication potential, global warming potential, ozone layer depletion potential, photochemical ozone creation potential, and terrestrial ecotoxicity potential for the DES to be larger than those for the CES.

The contributions of different phases to the environmental impacts for DES and CES are shown in Figure 4. It can be seen that, in addition to the ozone layer depletion potential, the environmental impacts for the DES and CES are mainly contributed by the usage phase. The construction phase for the DES and CES contributes the most to the ozone layer depletion potential, which accounts for 94.8% and 96.0%, respectively. Due to the recovery of metals, the impact of the system on human toxicity potential is effectively reduced in the demolition stage, leading to the minimal impact on the environment. Additionally, it is further illustrated that through metal recovery, the potential toxicity of DES and CES to human body is reduced by 10.1% and 4.1%, respectively, which is not shown in the figure due to its small value.

3.3 Endpoint analysis

The endpoint is based on various direct environmental impacts of the midpoint to further

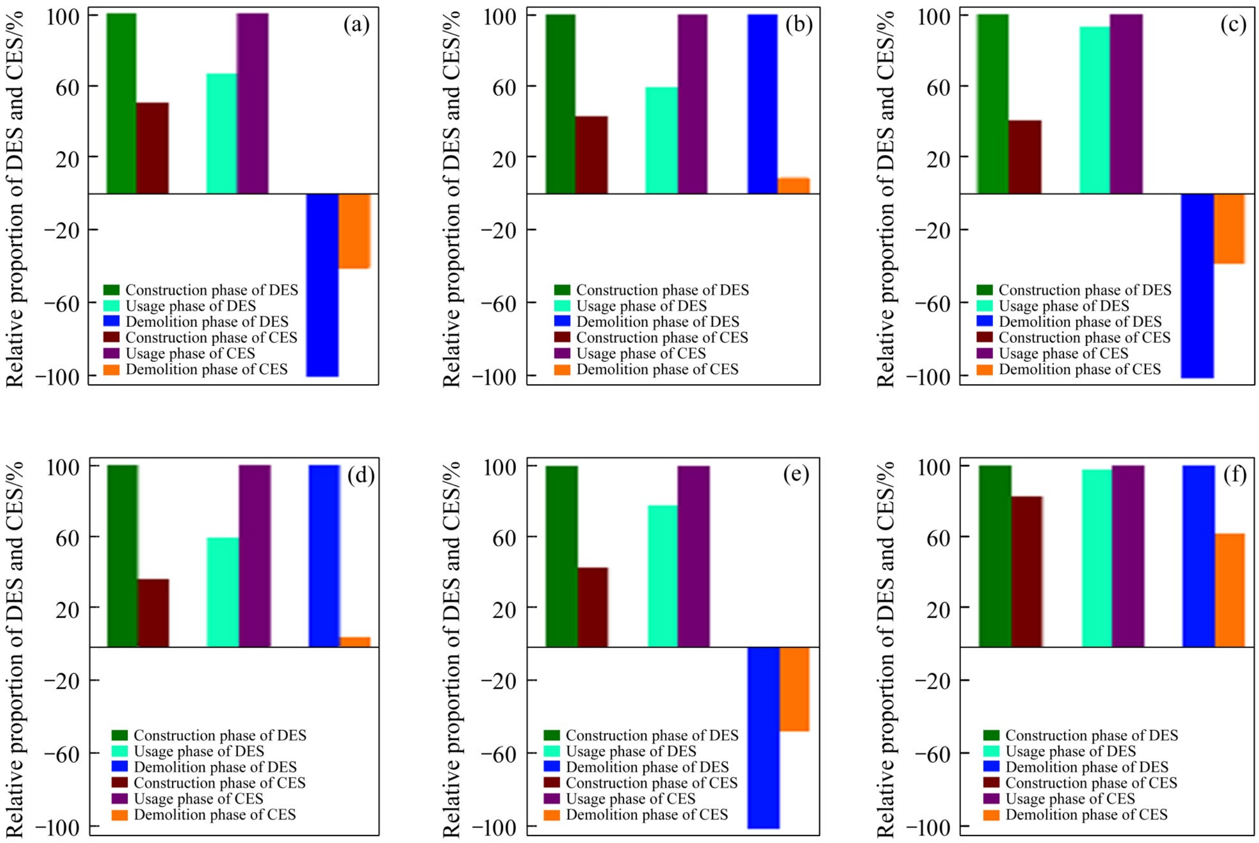

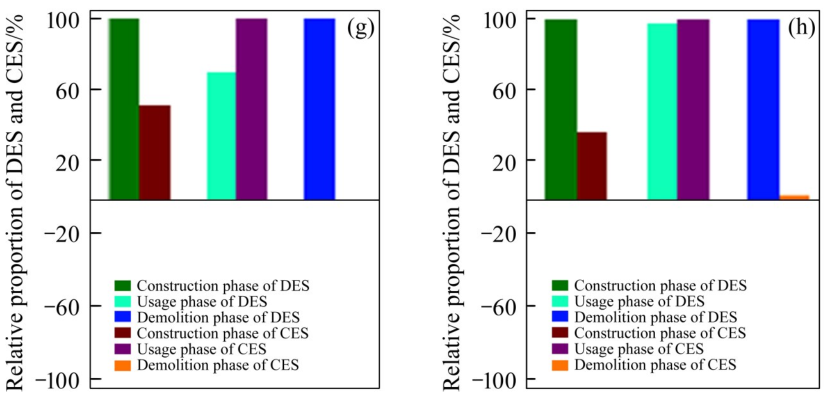

Figure 3 Environmental impact assessment for specific phases at the midpoint level: (a) AP; (b) EP; (c) FAETP; (d) GWP; (e) HTP; (f) ODP; (g) POCP; (h) TETP

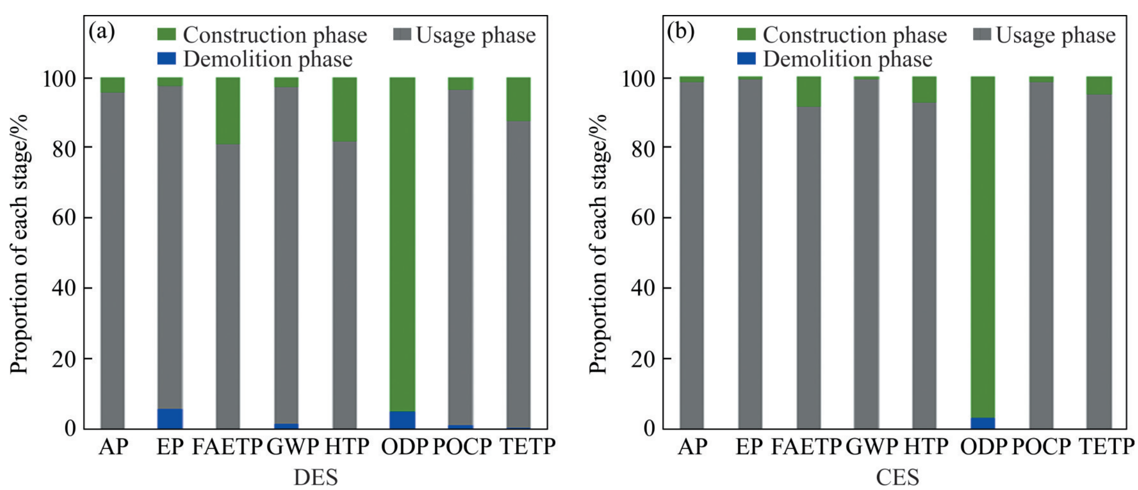

Figure 4 Contributions of different phases to the environmental impacts: (a) DES; (b) CES

classify the indirect and potential environmental impacts. The endpoint is used to deepen the analysis of the environmental impact. The endpoint tracks potential and indirect impacts and ultimately environmental consequences, which can distinguish environmental impacts more intuitively, explain phenomena more conveniently, and explore more clearly which environmental problems are caused. The disadvantage is that it is difficult to standardize and calculate weights for the endpoint. The panel, a method by using data to calculate weights in the Gabi 8 software, was employed to standardize and calculate weights for the endpoints in this study. Comparative total impact analysis and comparative phase impact analysis are discussed in this section.

3.3.1 Comparative total impact analysis

The endpoint level life-cycle performance of the DES and CES is shown in Table 2, which includes two categories: ecosystem quality and human health. Here, the damage to the ecosystem quality can be expressed as the relative decrease in the number of species (fraction)*area*time and the damage to human health is expressed as disability-adjusted life years (DALY). The ecosystem quality includes acidification and ecotoxicity. The human health includes carcinogenic effects, climate change, ozone layer depletion, radiation, inhalable inorganic matter, and inhalable organic matter. It can be found that the carcinogenic effects and ozone layer depletion for the DES are higher than those for the CES. The CES to DES indicator ratios of carcinogenic effects and ozone layer depletion are 0.7 and 0.8, respectively. The ecotoxicity for the DES is basically in agreement with that for the CES. It can be seen from the indicator ratio in Table 2 that the rest of the indicators for the DES are smaller than those for the CES. This is due to the use of renewable energy in the life-cycle of the DES system, which reduces its use of fossil energies such as natural gas.

The environmental performances for the DES and CES in terms of ecosystem quality and human health are illustrated in Figure 5. Due to the utilization of renewable energy, the ecosystem qualities for the DES and CES are 1.11×10^5 PDF*m^2*a and 1.43×10^5 PDF*m^2*a. The ecosystem quality for the DES decreased by 22.1% compared with that of the CES. The human health values for the DES and CES are 3.12DALY and 4.37DALY.

The comparative damage to ecosystem quality and human health for the DES and CES is shown in Figure 6. The damage to ecosystem quality for the DES and CES takes into account the emissions of SO_2 and NO_x that fall to the ground with the acid rain. This leads to land acidification and eutrophication. The acidification and ecotoxicity for the DES are 5.01×10^4 PDF*m^2*a and 6.11×10^4 PDF*m^2*a, which account for 45.1% and 55.0%, respectively. The acidification and ecotoxicity for the CES are 8.19×10^4 PDF*m^2*a and 6.07×10^4 PDF*m^2*a, respectively. The acidification for the DES is lower than that for the CES. However, the ecotoxicity for the DES is higher than that for the CES. The reason for this difference is the different energy consumption structure. In addition to the renewable energy, the DES consumes more electricity from the grid and less natural gas than the CES. Thus, the impact on the ecosystem quality has different effects.

Human health is mainly threatened by inhalable inorganic matter and climate change.

Table 2 Environmental performance at the endpoint level

Performance	Unit	Damage	CES	DES	CES/ DES
EQ	PDF*m^2*a	AC	8.19×10^4	5.01×10^4	1.6
		EC	6.07×10^4	6.07×10^4	1.0
HH	DALY	CE	4.94×10^{-2}	6.86×10^{-2}	0.7
		CC	1.25	0.768	1.6
		OLD	2.96×10^{-7}	3.59×10^{-7}	0.8
		RA	2.90×10^{-4}	2.33×10^{-4}	1.2
		IR	3.07	2.28	1.3
		OR	1.09×10^{-3}	8.55×10^{-4}	1.3

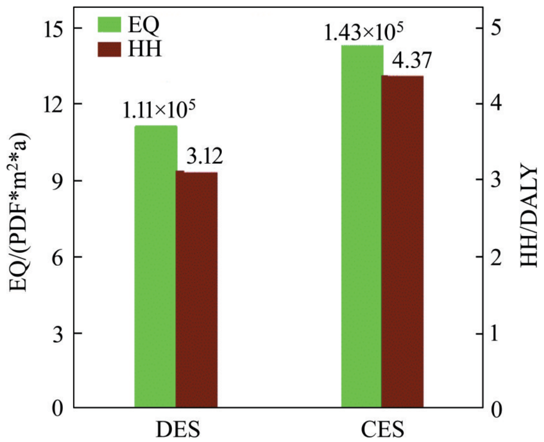

Figure 5 Environmental performance for the DES and CES

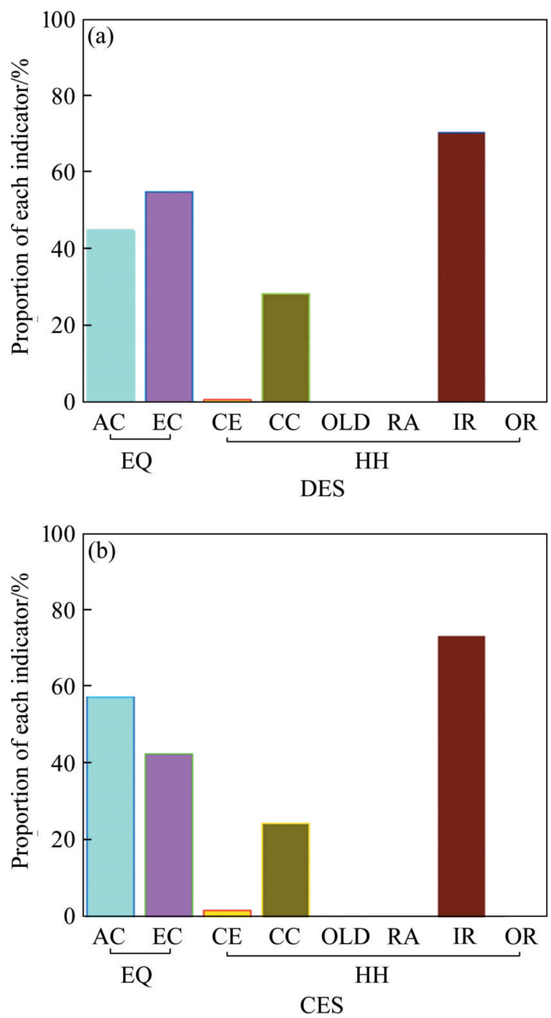

Figure 6 Comparative results for damage to ecosystem quality and human health from the DES (a) and CES (b)

Ozone layer depletion, radiation, and inhalable organic matter of the DES and CES have little influence on human health. The inhalable inorganic matter and climate change for the DES are 2.28DALY and 0.77DALY, which account for 73.1% and 24.7%, respectively. The inhalable inorganic matter and climate change for the CES are 3.07DALY and 1.25DALY, which account for 70.3% and 28.5%, respectively. The inhalable inorganic matter and climate change figures for the DES are both smaller than those for the CES. The inhalable inorganic matter mainly comes from the particulate matter discharged into the air from the natural gas combustion and power production. The natural gas consumption of the DES is less than that of the CES, which results in the inhalable inorganic matter for the DES being 0.79DALY less than that of the CES. The greenhouse gas (GHG) emissions lead to climate change. The renewable energy utilization in the DES can reduce the GHG emissions, which leads to the climate change caused by the DES being 0.48DALY less than that for the CES.

3.3.2 Comparative phase impact analysis

The environmental impacts for the DES and CES in the construction, usage, and demolition phases are illustrated in Figure 7. The indicators for the DES in the construction phase are higher than those for the CES. However, the indicators for the DES in the usage phase are smaller than those for the CES, especially in respect of climate change, which is only 60% for the DES compared with that for the CES. In the demolition phase, metal recovery reduces the environmental impact and produces deduction benefits. These results for endpoint level assessment are similar to those found for midpoint level assessment. The acidification for the DES is negative but that for the CES is positive in the demolition phase. This indicates that the metal recovery for the DES in the demolition phase is larger than that of the CES. This can reduce the discharge of industrial wastewater from metal production and the damage to the eutrophication of water bodies for the DES in comparison with the CES.

Figure 8 presents the contributions of the three phases to environmental damage, where ecosystem quality and human health are employed as the indicators. The usage phase contributes the most to the two indicators, which accounts for more than 95%. In the construction phase, the ecosystem quality and human health for the DES are both 2.9% higher than those for the CES. This is the result of

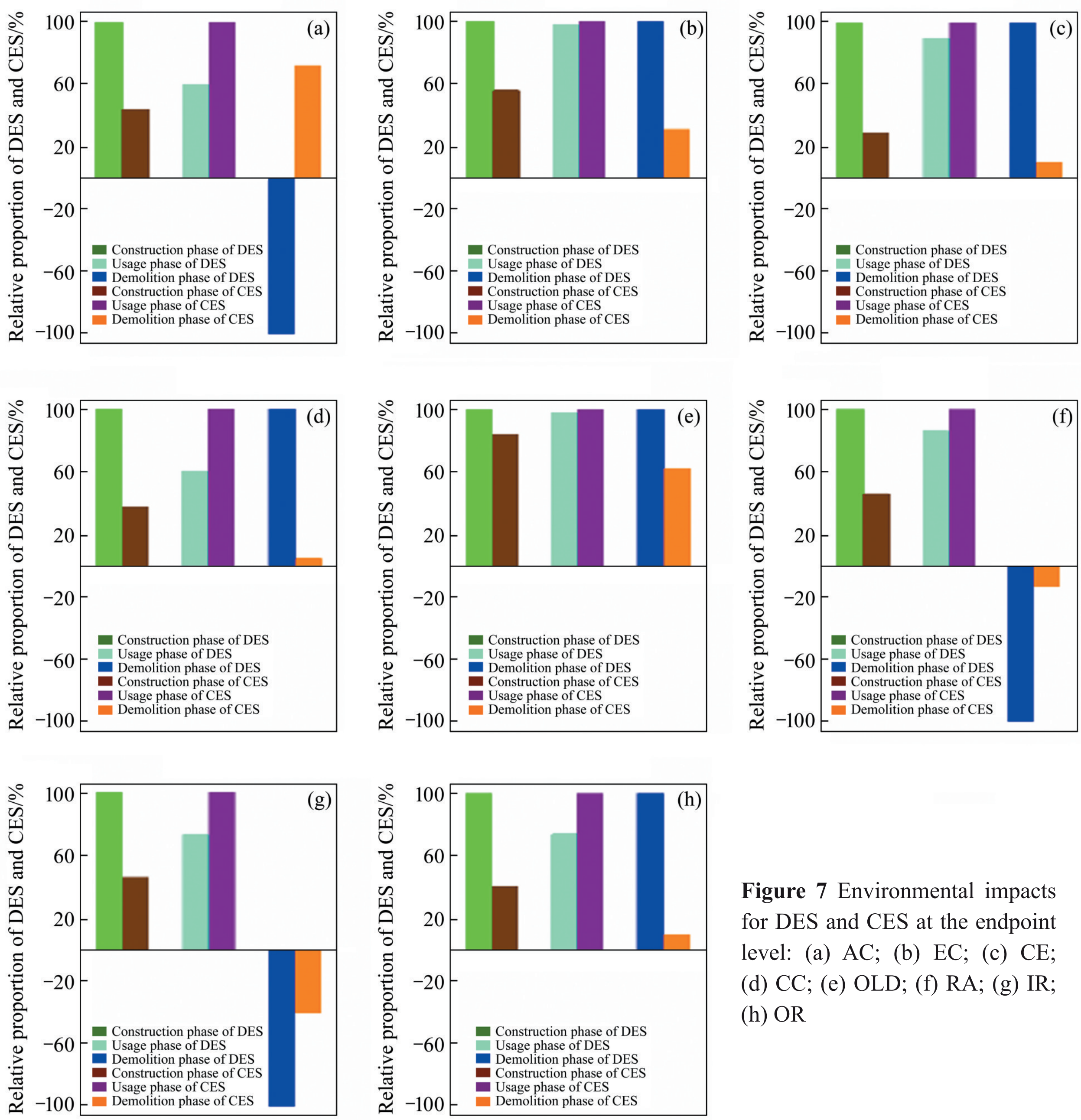

Figure 7 Environmental impacts for DES and CES at the endpoint level: (a) AC; (b) EC; (c) CE; (d) CC; (e) OLD; (f) RA; (g) IR; (h) OR

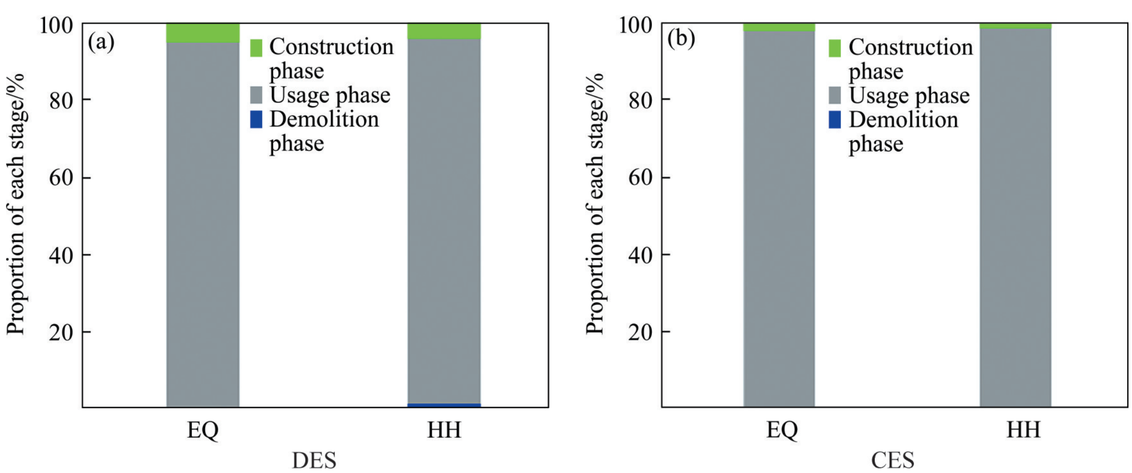

Figure 8 Contributions of DES (a) and CES (b) to environmental damage

the higher raw material and energy consumption for the DES in this phase. The ecosystem quality and human health in the demolition phase for the DES are −0.3% and 0.2%, respectively. The ecosystem quality and human health for the CES are negative in the demolition phase, which account for −0.1% and −0.04%, respectively. The negative value represents the offset benefit due to the metal recovery. It can also be found that the ecosystem quality and human health in the demolition phase are far lower than those in the usage phase. This indicates that the promotion of ecosystem quality and human health performance should focus on the optimization of the usage phase.

3.4 Hots-pot and sensitivity analysis for DES

On the basis of the midpoint and endpoint comparison of the DES and CES, it can be concluded that the life-cycle performance of the CES is lower than that of the DES in the construction and demolition phases. Due to the renewable energy utilization, the DES shows a better life-cycle performance in the usage phase compared to the CES. However, the performance of the usage phase plays a major role in the whole life-cycle performance. In a comprehensive comparison, the life-cycle performance of the DES is better than that of the CES. In order to investigate the life-cycle hots-pot and provide potential modifications to improve the environmental impacts of the DES, the hots-pot and sensitivity analyses for DES are studied separately in this section.

3.4.1 Hots-pot analysis

From the analysis in the former section, it can be determined that human health is mainly threatened by inhalable inorganic matter and climate change. The contributions of the different phases of the DES to environmental damage caused by climate change and inhalable inorganic matter are shown in Figure 9. It can be seen that the human health threat is mainly caused by the usage phase. The climate change values in the construction phase, usage phase, and demolition phase are 2.7%, 96.1%, and 1.3%, respectively. The inhalable inorganic matter released in the construction phase and usage phase is 3.3% and 96.7%, respectively. It is −0.3% in the demolition phase, which is not shown in the figure due to the small data.

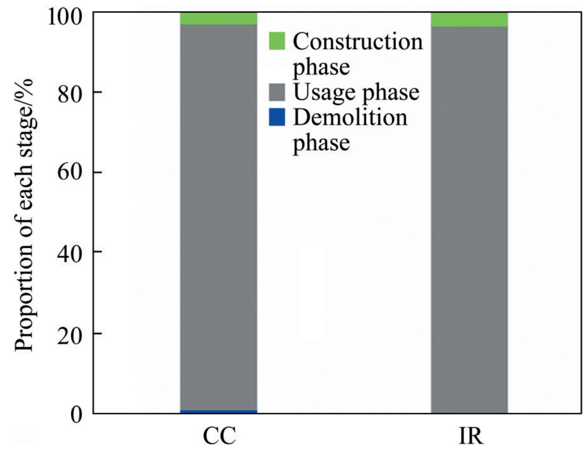

Figure 9 Contributions of the different phases of the DES to the environmental damage caused by climate change and inhalable inorganic matter

In order to simplify this study, the energy consumption caused by the system operation is considered and the energy consumption caused by other factors, such as system maintenance, is ignored. Figure 10 shows the contributions of the energy consumption to climate change and inhalable inorganic matter in the DES usage phase. The inhalable inorganic matter contents caused by the usage of electricity, natural gas, and tap water are 65.0%, 34.6%, and 0.5%, respectively. It can be seen that more than 98% climate change and inhalable inorganic matter are caused by the consumption of electricity and natural gas. It is considered that the inhalable inorganic matter content is mainly caused by particulate matter emissions in the electric power production process. The climate change caused by the usage of electricity, natural gas, and tap water is 34.3%, 63.8%, and 1.9%, respectively. The GHG emissions are caused by natural gas combustion, which most obviously influences the climate change. As power is generated from the coal-fired power plants, the power production process has a large number of emissions, leading to climate impact from the perspective of life cycle. The use of natural gas directly leads to greater greenhouse gas emissions, so it has a great impact on climate change. Therefore, controlling particulate matter emissions in power production and GHG emissions in the natural gas combustion process is important in order to reduce the human health damage caused by the DES.

3.4.2 Sensitivity analysis

There is a tradeoff between natural gas and

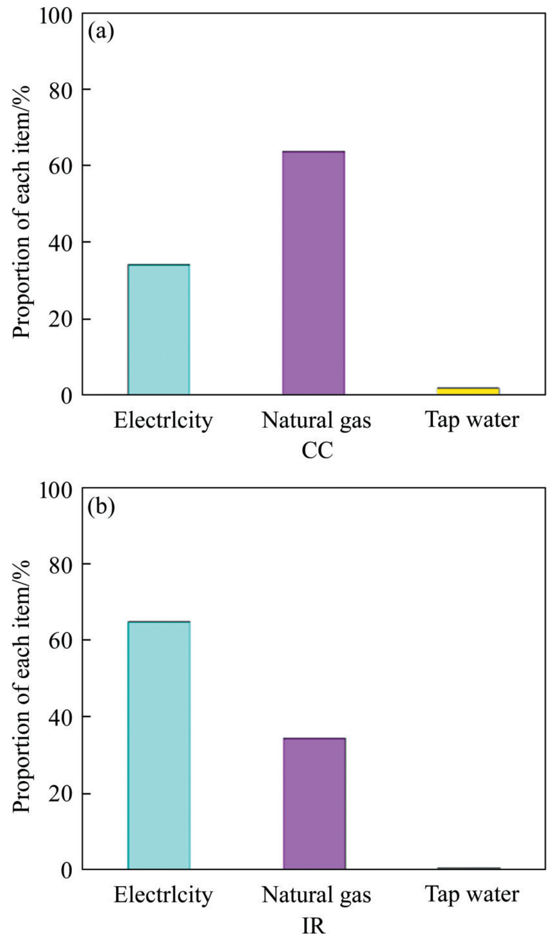

Figure 10 Contributions of the energy consumption to the environmental damage of CC (a) and IR (b)

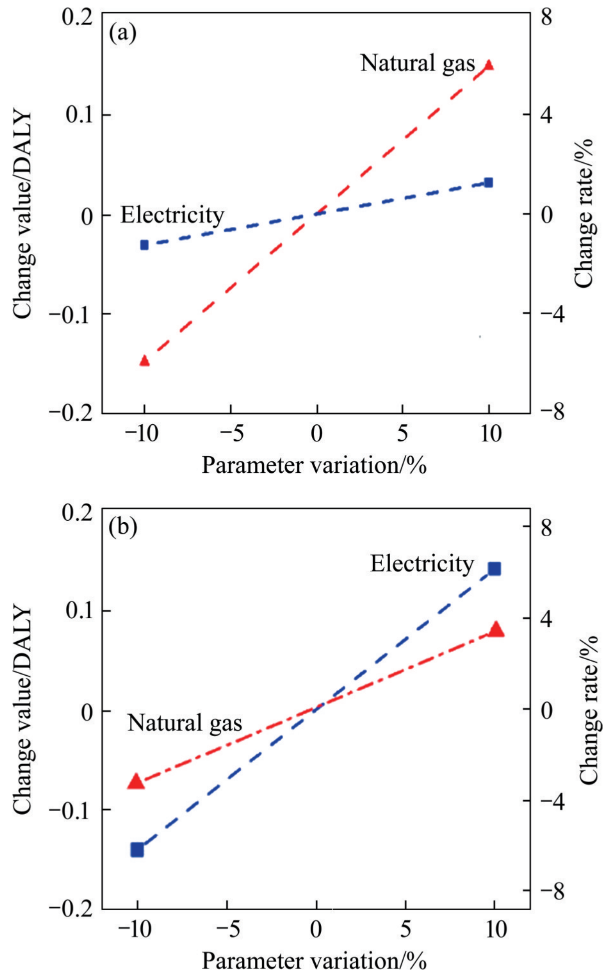

Figure 11 Influences of energy consumption on CC (a) and IR (b) in DES

electricity consumption. The sensitivity analysis of electricity and natural gas consumption was investigated, as shown in Figure 11. The sensitivity of electricity and natural gas varies from −10% to 10%. The CC and IR increase by 0.03DALY and 0.15DALY, respectively as the electricity increases by 10%. The corresponding change rates are 1.3% and 6.1%, respectively. As the natural gas increases by 10%, the CC and IR will increase by 0.15DALY and 0.08DALY. The corresponding change rates are 6.3% and 3.4%, respectively. Conversely, as the consumption of electricity and natural gas is reduced by 10%, the negative effects of CC and IR will also reduce the same values. It can be concluded that CC is significantly influenced by natural gas consumption and IR is significantly affected by electricity consumption.

4 Conclusions

In this study, we conducted a life-cycle comparison of DES and CES at a midpoint level and endpoint level. The life-cycle performance of the CES was lower than that of the DES in the construction and demolition phases and the DES showed a better life-cycle performance in the usage phase compared to the CES. In a comprehensive comparison, the life-cycle performance of the DES was found to be better than that of the CES at the midpoint level and endpoint level.

The life-cycle ‘hots-pot’ was identified and a sensitivity analysis was conducted for the DES. The results show that the human health threat was mainly caused in the usage phase due to the energy consumption. The human health threat ratio for the usage phase compared to the whole life-cycle was more than 95%. The ecosystem quality and human health for the DES were both 2.9% higher than those for the CES in the construction phase. The ecosystem quality and human health in the demolition phase for the DES were −0.3% and

0.2%, respectively. The ecosystem quality and human health for the CES were negative in the demolition phase, which account for −0.1% and −0.04%, respectively. The CES to DES indicator ratios of carcinogenic effects and ozone layer depletion were 0.7 and 0.8, respectively. The ecotoxicity for DES was basically in agreement with that for the CES. The rest of the indicators for the DES were smaller than those for CES. The CES to DES indicator ratios for acidification, climate change, radiation, inhalable inorganic matter, and inhalable organic matter were 1.6, 1.6, 1.2, 1.3 and 1.3, respectively. The inhalable inorganic matter released in the construction phase, usage phase, and demolition phase was 3.3%, 96.7% and −0.3%, respectively. The climate change in the construction phase, usage phase, and demolition phase was 2.7%, 96.1%, and 1.3%. The sensitivity analysis further suggests that the environmental damage caused by the DES can be reduced by the optimization of the natural gas and electricity consumption.

The research content of this paper focuses on the environmental impact of DES life-cycle. Due to the limitation of space and key content, only the hots-pot analysis and sensitivity analysis of inhalable inorganic matter and climate change are carried out. The energy structure of the system will be further studied to analyze the impact of energy consumption at all stages of its life-cycle in the future.

Table A1 The mass-energy life cycle inventory for DES and CES

Phase	Input/Output		Unit	DES	CES
Construction phase	Input (Material)	ABS	kg	11[a]	11[a]
		Aluminium	kg	353[a]	88[a]
		Cast iron	kg	761[a]	455[a]
		Copper pipe	kg	1,056[a]	0[a]
		Copper sheet	kg	410[a]	313[a]
		EPDM	kg	166[a]	162[a]
		Glass wool	kg	140[a]	140[a]
		PE	kg	764[a]	0[a]
		PP	kg	32[a]	32[a]
		PVC	kg	618[a]	479[a]
		Steel galvanized	kg	1776[a]	443[a]
		Steel plate	kg	880[a]	880[a]
		Stainless steel (304)	kg	1513[a]	1,199[a]
		Stainless steel (316)	kg	304[a]	273[a]
		Concrete	t	84[a]	9[a]
		Glass	kg	1584[a]	0[a]
	Input (Energy)	Diesel	kg	4583[a]	361[a]
		Electricity	kW·h	42800[a]	20600[a]
		Tap water	t	20[a]	4[a]
Usage phase	Input	Electricity	kW·h/a	69161[b]	70489[b]
		Natural gas	m^3/a	50215[b]	103206[b]
		Tap water	t/a	8213[b]	8213[b]
	Output	Cooling supply	GJ/a	121.54[b]	121.54[b]
		Heat supply	GJ/a	939.94[b]	939.94[b]
Demolition phase	Output	Recycled aluminium	kg	335[c]	84[c]
		Recycled copper	kg	1319[c]	282[c]
		Recycled steel	kg	4026[c]	2,516[c]
		Landfilling	t	93.28[c]	10.96[c]

[a] Source: statistics data. [b] Source: TRNSYS simulation result. [c] Source: Gabi simulation result.

Table A2 Calculated inputs of life-cycle inventory of DES and CES

Category	Subcategory/Unit	CES	DES
Nonrenewable energy	Crude oil/t	22.67	23.42
	Hard coal/t	455.61	451.17
	Lignite/t	4.53	3.75
	Natural gas/t	1970	967
	Peat/kg	53.94	32.93
	Uranium/kg	0.87	0.80
	Basalt/kg	8.50	10.92
	Bauxite/t	0.30	0.63
	Bentonite/t	2.48	1.25
	Chromium ore (39%)/kg	35.53	43.74
Nonrenewable resources	Clay/t	2.16	6.98
	Colemanite ore/kg	36.35	36.89
	Ore (copper, gold, silver)/t	0.12	1.16
	Dolomite/t	0.67	0.44
	Fluorspar/kg	41.88	50.09
	Gypsum (natural gypsum)/t	459.03	778.68
	Heavy spar ($BaSO_4$)/kg	1.38	2.02
	Ilmenite (titanium ore)/kg	2.71	3.35
	Inert rock/t	6.04×10^6	3.55×10^6
	Iron ore (56.86%)/t	995.27	1235.44
	Kaolin ore/kg	7.54	3.99
	Limestone (calcium carbonate)/t	4.86×10^4	5.30×10^4
	Magnesite/kg	13.76	125.63
	Magnesium chloride leach (40%)/t	595.89	595.14
	Manganese ore (R.O.M.)/kg	28.13	35.01
	Molybdenite (Mo 0.24%)/kg	11.27	13.88
	Natural aggregate/t	44.33	99.37
	Natural pumice/kg	5.61	3.31
	Nickel ore (1.6%)/kg	5.23	6.44
	Ore mined/t	0.00	18.12
	Phonolite/kg	6.55	6.55
	Potassium chloride/kg	0.50	0.64
	Quartz sand/kg	35.43	39.05
	Shale/kg	43.82	25.01
	Sodium chloride (rock salt)/kg	1.20	1.68
	Soil/t	0.71	6.39
	Stone from mountains/kg	25.28	37.61
	Carbon dioxide/kg	29.25	27.75
Renewable resources	Water/t	44.33	99.37
	Air/t	9.85	9.72
	Forest, primary/kg	13.13	37.13
	Renewable fuels/kg	90.23	110.82
	Nitrogen/kg	36.60	177.09
	Oxygen/kg	185.68	364.69
	Potato (t100)/kg	0.43	0.53

Table A3 Calculated outputs of Life-cycle inventory of DES and CES

Category	Subcategory/Unit	CES	DES
Waste (stock)	Low radioactive wastes/kg	3.17	2.84
	Medium radioactive wastes/kg	1.35	1.21
	Radioactive tailings/kg	177.94	161.47
	Overburden/t	1941.59	7556.53
	Spoil/t	28.65	36.16
	Tailings/t	42.48	42.50
	Waste/t	36.06	101.46
Heavy metals to air	Sb/kg	1.06	1.06
	As/kg	0.59	0.60
	Cr/kg	1.91	1.91
	Co/kg	0.63	0.63
	Cu/kg	1.02	0.99
	Pb/kg	4.48	4.45
	Mn/kg	25.11	25.01
	Ni/kg	3.24	3.25
	Se/kg	0.47	0.63
	Sn/kg	14.28	14.25
	V/kg	3.26	3.25
	Zn/kg	5.42	5.41
Inorganic emissions to air	Ammonia (NH_3)/kg	11.53	11.53
	Barium (Ba)/kg	12.56	12.53
	Boron compounds/kg	2.72	2.70
	Bromine (Br)/kg	1.60	1.60
	Carbon dioxide (CO_2)/t	5.62×10^3	3.42×10^3
	Carbon monoxide (CO)/t	2.19	1.97
	Chlorine (Cl)/kg	0.67	0.69
	Copper sulfate ($CuSO_4$)/kg	0.00	0.71
	Hydrogen(H)/kg	5.53	15.43
	Hydrogen chloride (HCl)/kg	35.87	35.51
	Hydrogen fluoride (HF)/kg	2.72	2.73
	Hydrogen sulfide (H_2S)/kg	7.17	3.93
	Nitrogen (N_2)/kg	609.73	393.20
	Nitrogen dioxide (NO_2)/t	9.09	4.43
	Nitrogen oxides (NO_x)/t	40.18	42.82
	Oxygen (O_2)/kg	765.18	701.96
	Sulphur dioxide (SO_2)/kg	6393.33	4852.64
	Sulfuric acid(H_2SO_4)/kg	0.50	0.91
	Water (evapotranspiration)/t	6.52×10^3	6.34×10^3
	Water vapor/t	1.11×10^4	1.05×10^4
Organic emissions to air	NMVOC/t	1.12	0.72
	Hydrocarbons/kg	3.90	7.65
	Particles to air/kg	4.00	3.66
	Methane/t	14.79	10.90
Other emissions to air	Other emissions/t	5507.08	5467.80

to be continued

Contined

Category	Subcategory/Unit	CES	DES
Heavy metals to fresh water	Cr/kg	0.87	0.89
	Fe/kg	11.90	9.66
	Mn/kg	0.71	0.73
	Mo/kg	0.51	0.61
	Zn/kg	0.33	5.64
Inorganic emissions to fresh water	Aluminum (Al)/kg	1.27	1.25
	Ammonium (NH_3)/kg	11.50	26.26
	Barium (Ba)/kg	0.73	0.72
	Boron (B)/kg	4.05	4.03
	Calcium (Ca)/kg	503.39	553.17
	Carbonate ($CaCO_3$)/kg	45.64	45.43
	Chlorine (Cl)/kg	8.73	8.63
	Cl (dissolved)/kg	0.86	0.77
	Fluoride/kg	14.39	12.68
	Magnesium (Mg)/kg	95.48	95.33
	Nitrate/kg	81.20	79.74
	Nitrogen/kg	9.06	8.51
	Phosphate/kg	1.40	1.29
	Phosphorus/kg	4.45	5.74
	Potassium/kg	15.69	16.00
	Sodium/t	0.36	0.32
	Sodium chloride (rock salt)/kg	0.96	0.56
	NaClO/kg	11.53	11.57
	Na_2SO_4/kg	6.90	6.69
	Strontium/kg	2.50	2.40
	Sulfate/t	0.40	0.39
	Sulfide/kg	8.26	8.30
	Sulfite/kg	0.96	0.95
Organic emissions to fresh water	Methanol/kg	0.84	0.84
	Oil/kg	4.24	3.12
	Carbon, organically bound/kg	85.38	73.13
	Organic compounds/kg	22.14	22.26
Other emissions to fresh water	Collected rainwater/t	25.59	83.94
	Cooling water/t	2.20×10^{4}	2.15×10^{4}
	Processed water/kg	4.75×10^{3}	4.72×10^{3}
	Turbined water/t	1.10×10^{6}	1.00×10^{6}
Particles to fresh water	Particles/kg	6.40	3.71
Radioactive emissions to fresh water	Ra226/t	1.44×10^{4}	1.32×10^{4}
Inorganic emissions to sea water	Carbonate/kg	13.11	9.88
	Chloride/kg	1.06×10^{3}	7.86×10^{2}
	Nitrate/kg	0.52	0.59
	Sodium/kg	19.54	9.61

to be continued

Contined

	Subcategory/Unit	CES	DES
Inorganic emissions to sea water	Sulphate/kg	5.55	4.17
	Sulfide/kg	2.39	1.80
Organic emissions to sea water	Hydrocarbons/kg	0.67	0.49
Other emissions to sea water	Cooling water/t	1.69×10^4	8.70×10^3
	Processed water/t	4.45	5.64
	Waste water/kg	1.84	2.09
Particles to sea water	Solids (suspended)/t	0.78	0.38
Inorganic emissions to industrial soil	Ammonia/kg	11.60	99.14
	Calcium/kg	6.69	56.61
	Chloride/kg	12.54	44.06
	Fluoride/kg	0.09	0.69
	Magnesium/kg	0.94	8.06
	Phosphorus/kg	0.93	7.98
	Potassium/kg	1.93	16.45
	Sodium/kg	2.87	24.57
	Sulphate/kg	0.16	1.33
	Sulfide/kg	0.93	7.95

Contributors

The overarching research goals were developed by LIU Chang-rong, WANG Han-qing, and YANG Sheng. LIU Chang-rong and TANG Yi-fang provided the life-cycle inventory of the system, and analyzed the data. LI Chao-jun and JIN Wen-ting established the system LCA models. LIU Chang-rong, TANG Yi-fang and YANG Sheng analyzed the LCI results. The initial draft of the manuscript was written by LIU Zhi-qiang, LIU Chang-rong, and TANG Yi-fang. All authors replied to reviewers' comments and revised the final version.

Conflict of interest

The authors declare that they have no known competing financial interests or personal relationships that could have appeared to influence the work reported in this paper.

References

[1] Center TUBER. 2017 Annual report on China building energy efficiency [M]. Beijing: China Architecture & Building Press, 2018. (in Chinese)

[2] WANG Jiang-jiang, YANG Ying, MAO Tian-zhi, et al. Life cycle assessment (LCA) optimization of solar-assisted hybrid CCHP system [J]. Applied Energy, 2015, 146: 38−52. DOI: 10.1016/j.apenergy.2015.02.056.

[3] SOMMA M D, YAN B, BIANCO N, et al. Multi-objective design optimization of distributed energy systems through cost and exergy assessments [J]. Applied Energy, 2017, 204: 1299−1316. DOI: 10.1016/j.apenergy.2017.03.105.

[4] JING You-yin, BAI He, WANG Jiang-jiang, et al. Life cycle assessment of a solar combined cooling heating and power system in different operation strategies [J]. Applied Energy, 2012, 92: 843−853. DOI: 10.1016/j.apenergy.2011.08.046.

[5] AL-SULAIMAN F A, HAMDULLAHPUR F, DINCER I. Performance assessment of a novel system using parabolic trough solar collectors for combined cooling, heating, and power production [J]. Renewable Energy, 2012, 48: 161−172. DOI: 10.1016/j.renene.2012.04.034.

[6] RAD F M, FUNG A S, LEONG W H. Feasibility of combined solar thermal and ground source heat pump systems in cold climate, Canada [J]. Energy and Buildings, 2013, 61: 224−232. DOI: 10.1016/j.enbuild.2013.02.036.

[7] LIU Tai-xiu, LIU Qi-bin, LEI Jing, et al. Solar-clean fuel distributed energy system with solar thermochemistry and chemical recuperation [J]. Applied Energy, 2018, 225: 380−391. DOI: 10.1016/j.apenergy.2018.04.133.

[8] FANI M, SADREDDIN A. Solar assisted CCHP system, energetic, economic and environmental analysis, case study: Educational office buildings [J]. Energy and Buildings, 2017, 136: 100−109. DOI: 10.1016/j.enbuild.2016.11.052.

[9] LIU Tai-xiu, LIU Qi-bin, DA Xu, et al. Performance investigation of a new distributed energy system integrated a solar thermochemical process with chemical recuperation [J]. Applied Thermal Engineering, 2017, 119: 387−395. DOI: 10.1016/j.applthermaleng.2017.03.073.

[10] YILMAZ F. Thermodynamic performance evaluation of a novel solar energy based multigeneration system [J]. Applied Thermal Engineering, 2018, 143: 429−437. DOI: 10.1016/j.applthermaleng.2018.07.125.

[11] ZOGOU O, STAMATELOS A. Optimization of thermal performance of a building with ground source heat pump system [J]. Energy Conversion and Management, 2007, 48(11): 2853−2863. DOI: 10.1016/j.enconman.2007.07.012.
[12] WANG En-yu, FUNG A S, QI Cheng-ying, et al. Performance prediction of a hybrid solar ground-source heat pump system [J]. Energy and Buildings, 2012, 47: 600−611. DOI: 10.1016/j.enbuild.2011.12.035.
[13] OZGENER O, HEPBASLI A. A review on the energy and exergy analysis of solar assisted heat pump systems [J]. Renewable and Sustainable Energy Reviews, 2007, 11(3): 482−496. DOI: 10.1016/j.rser.2004.12.010.
[14] OZGENER O, HEPBASLI A. Modeling and performance evaluation of ground source (geothermal) heat pump systems [J]. Energy and Buildings, 2007, 39(1): 66−75. DOI: 10.1016/j.enbuild.2006.04.019.
[15] KJELLSSON E, HELLSTRÖM G, PERERS B. Optimization of systems with the combination of ground-source heat pump and solar collectors in dwellings [J]. Energy, 2010, 35(6): 2667−2673. DOI: 10.1016/j.energy.2009.04.011.
[16] CHAPUIS S, BERNIER M. Seasonal storage of solar energy in borehole heat exchangers [C]// 11th Int. IBPSA Conf. Glasgow, Scotland, 2009J: 599−606. http://www.ibpsa.org/proceedings/BS2009/BS09_0599_606.pdf.
[17] OZGENER O. Use of solar assisted geothermal heat pump and small wind turbine systems for heating agricultural and residential buildings [J]. Energy, 2010, 35(1): 262−268. DOI: 10.1016/j.energy.2009.09.018.
[18] YUAN Jia-qi, XIAO Zi-wei, ZHANG Chong, et al. A control strategy for distributed energy system considering the state of thermal energy storage [J]. Sustainable Cities and Society, 2020, 63: 102492. DOI: 10.1016/j.scs.2020.102492.
[19] THIBODEAU C, BATAILLE A, SIÉ M. Building rehabilitation life cycle assessment methodology-state of the art [J]. Renewable and Sustainable Energy Reviews, 2019, 103: 408−422. DOI: 10.1016/j.rser.2018.12.037.
[20] JING You-yin, BAI He, WANG Jiang-jiang. Multi-objective optimization design and operation strategy analysis of BCHP system based on life cycle assessment [J]. Energy, 2012, 37(1): 405−416. DOI: 10.1016/j.energy.2011.11.014.
[21] ZHANG Di, EVANGELISTI S, LETTIERI P, et al. Optimal design of CHP-based microgrids: Multiobjective optimisation and life cycle assessment [J]. Energy, 2015, 85: 181−193. DOI: 10.1016/j.energy.2015.03.036.
[22] ANASTASELOS D, OXIZIDIS S, MANOUDIS A, et al. Environmental performance of energy systems of residential buildings: Toward sustainable communities [J]. Sustainable Cities and Society, 2016, 20: 96−108. DOI: 10.1016/j.scs.2015.10.006.
[23] OREGI X, HERNANDEZ P, HERNANDEZ R. Analysis of life-cycle boundaries for environmental and economic assessment of building energy refurbishment projects [J]. Energy and Buildings, 2017, 136: 12−25. DOI: 10.1016/j.enbuild.2016.11.057.
[24] MOSLEHI S, REDDY T A. An LCA methodology to assess location-specific environmental externalities of integrated energy systems [J]. Sustainable Cities and Society, 2019, 46: 101425. DOI: 10.1016/j.scs.2019.101425.
[25] ALBERTÍ J, RAIGOSA J, RAUGEI M, et al. Life cycle assessment of a solar thermal system in Spain, eco-design alternatives and derived climate change scenarios at Spanish and Chinese national levels [J]. Sustainable Cities and Society, 2019, 47: 101467. DOI: 10.1016/j.scs.2019.101467.
[26] HAJARE A, ELWAKIL E. Integration of life cycle cost analysis and energy simulation for building energy-efficient strategies assessment [J]. Sustainable Cities and Society, 2020, 61: 102293. DOI: 10.1016/j.scs.2020.102293.
[27] BRUSSEAU M L. Sustainable development and other solutions to pollution and global change [M]// Environmental and Pollution Science. Amsterdam: Elsevier, 2019: 585−603. DOI: 10.1016/b978-0-12-814719-1.00032-x.
[28] ISO14040. Environmental management-life cycle assessment-principles and framework [S]. 2006.
[29] ISO14044. Environmental management-life cycle assessments-requirements and guidelines [S]. 2006.
[30] Think step. GaBi 8 software and databases [M]. Germany: Leinfelden-Echterdingen, 2018.
[31] YU Sui-ran, TAO Jing. Product life cycle design and evaluation [M]. Beijing: Science Press, 2012. (in Chinese)
[32] GUINEE J B. Handbook on life cycle assessment operational guide to the ISO standards [J]. The International Journal of Life Cycle Assessment, 2002, 7(5): 311−313. DOI: 10.1007/BF02978897.
[33] POHL J, HILTY L M, FINKBEINER M. How LCA contributes to the environmental assessment of higher order effects of ICT application: A review of different approaches [J]. Journal of Cleaner Production, 2019, 219: 698–712. DOI: 10.1016/j.jclepro.2019.02.018.
[34] GOEDKOOP M, SPRIENSMA R. The ecoindicator-99, a damage oriented method for life cycle impact assessment; reportmethodology, amersfoort, pré consultants [R]. Vrom Zoetermeer, 2000.
[35] HOFSTETTER P. Perspective in life cycle impact assessment: A structured approach to combine of the technosphere, ecosphere and valuesphere [J]. The International Journal of Life Cycle Assessment, 2000, 5(1): 58. DOI: 10.1007/BF02978561.
[36] LIU Xin, YUAN Zeng-wei. Life cycle environmental performance of by-product coke production in China [J]. Journal of Cleaner Production, 2016, 112: 1292−1301. DOI: 10.1016/j.jclepro.2014.12.102.
[37] ALEJANDRE E M, van BODEGOM P M, GUINÉE J B. Towards an optimal coverage of ecosystem services in LCA [J]. Journal of Cleaner Production, 2019, 231: 714–722. DOI: 10.1016/j.jclepro.2019.05.284.
[38] LUAN Zhong-quan. Environmental attributes assessment of product green design and its application based on the eco-indicator 99 [J]. Light Industry Machinery, 2004(2): 8−11. (in Chinese)
[39] FINNVEDEN G, HAUSCHILD M Z, EKVALL T, et al. Recent developments in life cycle assessment [J]. Journal of Environmental Management, 2009, 91(1): 1−21. DOI: 10.1016/j.jenvman.2009.06.018.
[40] HUISMAN J. The QWERTY/EE concept, quantifying recyclability and eco-efficiency for end-of-life treatment of consumer electronic products [M]// Design Engineering & Production. 2003. https://www.researchgate.net/publication/27346227.

(Edited by YANG Hua)

中文导读

中国集中供热和制冷用分布式能源系统与常规能源系统生命周期的性能比较研究

摘要：分布式能源系统在单栋建筑制冷供热方面的应用受到高度重视，研究分布式能源系统的生命周期环境影响，对鼓励和引导中国分布式能源系统的发展具有重要意义。然而，关于分布式能源系统在建筑制冷供热过程中的环境性能全面分析的研究较少。本研究基于ISO14040-2006和ISO14044-2006标准，对分布式能源系统(DES)进行生命周期评价(LCA)，以常规能源系统(CES)为基准，量化其环境影响。采用GaBi 8软件进行生命周期评价。采用环境科学中心(CML)法和生态指数99(EI 99)法分别进行中点水平和终点水平的环境影响评价。结果表明：与CES相比，DES在使用阶段表现出更好的生命周期性能；在中点水平上，酸化潜力、富营养化潜力和全球变暖潜力的CES与DES指标比值分别为1.5、1.5和1.6，终点水平的生态系统质量和人类健康两类影响指标中，除致癌性和臭氧消耗指标外，CES和DES其他指标的比值均大于1，即从整个生命周期来看，DES的生命周期性能在中点和端点水平均优于CES；DES对人体健康的威胁主要是由于使用阶段的能源消耗造成的。敏感性分析表明，当电量增加10%时，气候变化和可吸入无机物变化幅度分别为1.3%和6.1%；当天然气增加10%时，气候变化和可吸入无机物分别增加6.3%和3.4%；通过天然气和电耗的优化，可以显著降低DES造成的人类健康威胁和环境破坏。

关键词：生命周期评价；分布式能源系统；常规能源系统；集中供热和制冷；环境影响